International Journal of Emerging Technology and Advanced Engineering
Website: www.ijetae.com (ISSN 2250-2459, ISO 9001:2008 Certified Journal, Volume 5, Issue 1, January 2015)

# Random Processes of Evolution of a Mobile Robot in an Unstructured Environment

Tony Stanescu[1], Valer Dolga[2]
[1]Phd., Politehnica University of Timisoara, Bd. Mihai Viteazu 1, Timisoara, Romania, cod 300222
[2]Prof. Dr. Eng., Politehnica University of Timisoara, Bd. Mihai Viteazu 1, Timisoara, Romania, cod 300222

***Abstract*— Evolution of the mobile robot is currently characterized by multiple applications in dynamic workspaces and low initial knowledge. In this paper presents aspects of approaching random processes of evolution of a mobile robot in an unstructured environment . The experimental results are used for modeling an infrared sensor (integrated in the mobile robot structure) and to assess the probability of locating obstacles in the environment.**

***Keywords*— Infrared sensor, Location, Mobile robot.**

## I. INTRODUCTION

Navigating mobile robots - autonomous mobile systems - is a broad subject, covering a broad spectrum of different technologies and applications [1], [2], [3].

Moving the mobile robot in a workspace (scene work) is affected by a number of phenomena, processes falling within the Random: ground contact, dynamic scene analysis, the size and shape of objects in the scene work [4]. These requirements vary greatly with the application. Any autonomous system must be able to determine its position at a resolution at least within its own dimensions, in order to navigate and interact correctly with the working environment [5].

Avoiding obstacles is one of the most important issues which arise from the realization of a mobile robot. Without this capability, the robot motion as restrictive and fragile.

Obstacle detection and avoidance of obstacles means stopping or changing direction of travel of the mobile robots, in order to avoid collisions. It is fundamental to the design of a mobile robot research, as it is equipped with a sensor that is capable of acquiring information on which to form an internal representation of the surrounding world, to make decisions and plan action.

Ultrasonic and infrared sensors are widely used in the construction of mobile robots [6], [7], [8].

Response amplitude sensors infrared (IR) is based on the reflection of optical radiation on the objects in the scene work.

Reflective process depends on the characteristics of the surface reflectance of the object. The response in the sensor elements (R) is widely used due to its low cost and fast response time. The response time of these sensory elements is superior ultrasonic sensors.

Everett [9] used to determine the phase difference of the received signal the location of objects. IR variants are various sensory elements. Sabatini [10] and Colla [11] uses an IR sensor for low fields (below 250 mm) with a resolution unconvincing. Vaz [12] uses an infrared sensor to an acceptable accuracy (5 mm) reflector system known positions. Korba [13] uses multiple sensory elements IR for determining the distance but the results are compelling.

Benet & all [14] state that documentation on the use of IR sensors in mobile robotics is reduced.

Mohammad [15] addresses the Phong lighting model to analyze IR sensors to determine distance continuing research in this area.

Research in the field aim to identify new variants both sensory (IR) to be integrated successfully in the construction of mobile robots and IR sensor behavior.

Novotny [16] analyzes the behavior of the sensing element on the energy emitted and received respectively. Determine the distance between the sensing element and the obstacle is evaluated by the authors in three steps: identification of the obstacle parameter identification and orientation of the plane of the element sensory refelexie the obstacle plan and calculate the distance between sensor and obstacle.

The paper aims to analyze the possibilities of using an infrared sensor for locating an object, the sensor characteristic determination and choice mathematical expression that describes this feature and illustrate through practical application of those stated.

The paper is divided into four chapters preceded by “Abstract” and ending with “Acknowledgments” and “References”. In the chapter "Determination of the characteristic of sensory element" is studied calculus characteristic feature direct and inverse variations are presented and adopted.

International Journal of Emerging Technology and Advanced Engineering
Website: www.ijetae.com (ISSN 2250-2459, ISO 9001:2008 Certified Journal, Volume 5, Issue 1, January 2015)

In the chapter "Locating an obstacle and experimental stand", the authors analyze the possibility to determine our location of an obstacle, the probability density of the random process considered and exemplified by cases. The paper ends with conclusions on the facts presented and Acknowledgments.

## II. Determination Of The Characteristic Of Sensory Element

For obstacle detection analysis and integration of sensory elements such structure a mobile robot using sensor Sharp GP2Y0A21YK, figure 1, [17].

**Fig. 1, Sensor Sharp GP2Y0A21YK**

Sensor element emits a beam of infrared radiation incidence. This is reflected by the obstacle and then is received by the sensor (Figure 2).

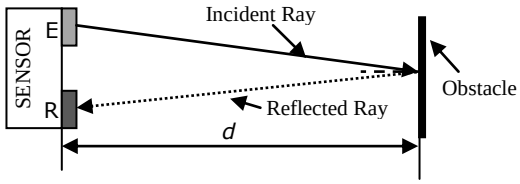


**Fig. 2, The working principle of the sensor IR**

Integrating and using the Sharp sensor GP2Y0A21YK becomes possible if known characteristic both direct

U = f(x), (U – output signal of sensor element; x – distance between sensor and target object) and inverse characteristic x = g(U). For this purpose it was developed stand whose scheme is shown in figure 3.

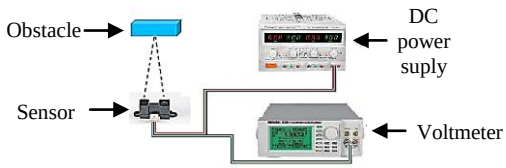


**Fig. 3. Scheme booth working**

The area investigated was placed obstacles paralelilpipedical and cylindrical shape. Reference distance between the sensor and obstacle was measured with a laser telemeter Bosch DLE 70 Professional.

The bench said the authors developed sets of measurements, and the results were statistically processed. Based on these values processed past the mathematical approximation of the characteristic.

### *A. Direct Characteristict*

For determine direct characteristic was used in the first step the position that allowed POLYVAL numerical evaluation of the polynomial approximation to a set of values of the input size and the error representation obtained [17].

Figure 4 shows the curve of polynomial approximation and in Table 1 the assessment of errors.

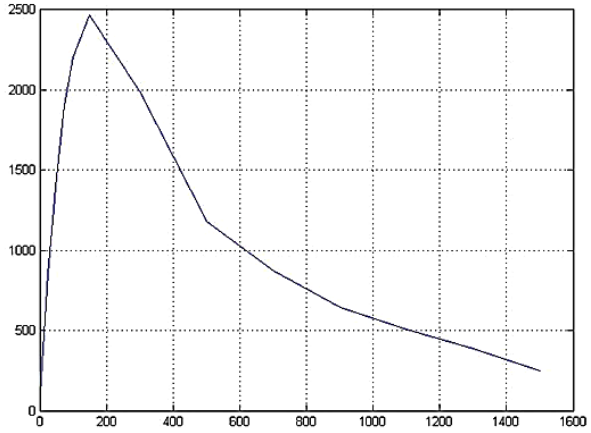


**Fig. 4, Sensory input feature SHARP**

**Table 1,**
**Evaluation errors**

| X [m] | Y [V] | f | Y-f |
|---|---|---|---|
| 0 | 0 | 0.0576 | -0.0576 |
| 0.0250 | 0.9527 | 0.8565 | 0.0962 |
| 0.0500 | 1.5635 | 1.4625 | 0.1010 |
| 0.0750 | 1.7492 | 1.9020 | -0.1528 |
| 0.1000 | 2.1050 | 2.2005 | -0.0955 |
| 0.1500 | 2.6067 | 2.4700 | 0.1367 |
| 0.2994 | 1.9549 | 1.9942 | -0.0393 |
| 0.5008 | 1.1942 | 1.1765 | 0.0177 |
| 0.7008 | 0.8617 | 0.8712 | -0.0095 |
| 0.9004 | 0.6500 | 0.6458 | 0.0042 |
| 1.1000 | 0.5066 | 0.5079 | -0.0013 |
| 1.2994 | 0.3874 | 0.3871 | 0.0003 |
| 1.5005 | 0.2497 | 0.2497 | -0.0000 |

International Journal of Emerging Technology and Advanced Engineering
Website: www.ijetae.com (ISSN 2250-2459, ISO 9001:2008 Certified Journal, Volume 5, Issue 1, January 2015)

The structure S contains the fields for the triangular factor (R) from QR decomposition of Vandermonde matrix of X, the degrees of freedom (df), and the norm of the residuals (normr) (Table 2), [18].

**Table 2,**
**Determining of the characteristic**

| | |
|---|---|
| *R* | 10 x 10 double |
| *df* | 3 |
| *normr* | 275.5191 |

In the next step was called the working environment Matlab/Cftool. [18]

In figure 5 is shown working the box mathematical approximation based on exponential functions with two terms of the form:

$$U = 3790 \cdot e^{-0.002034 \cdot x} - 3829 \cdot e^{-0.01696 \cdot x} \quad (1)$$

In an active textbox in figure 5 are presented and values of statistics characterizing the solution obtained and presented in Fig. 6 is characteristic element approximation sensory range [150...1500] mm.

Sensory element characteristic equation is described by the expression:

$$U = 2596 \cdot e^{-0.003762 \cdot x} + 1489 \cdot e^{-0.001114 \cdot x} \; [mV] \quad (2)$$

The results allow an analysis on the best result to be admitted as such. In Table 3 presents a comparison of the approximate statistical index refereritoare characteristic on [150 mm .... 1500 mm]. It is noted that the polynomial approximation is superior statistical indices exponential approximation.

Notations in the table are the following: SSE - sum of squared errors of prediction, R_square - coefficient of determination and RMSE - root-mean-square error.

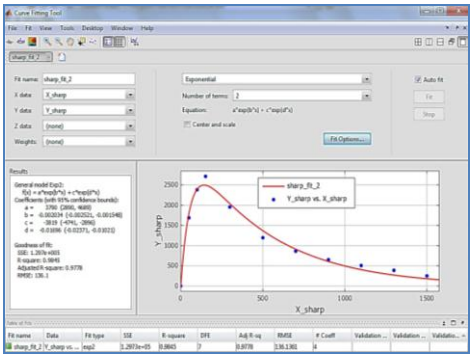

**Fig. 5, Characteristic approximation by an exponential function**

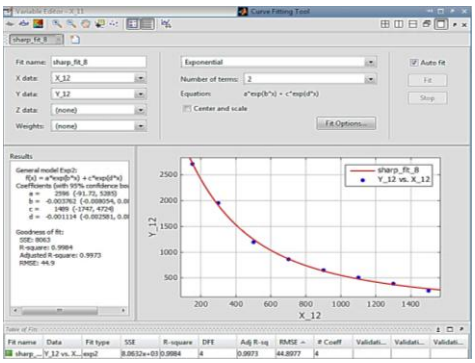

**Fig. 6. Characteristic element approximation sensory interval [150…1500] mm.**

**Table 3,**
**Approximating of the characteristic**

| | Approximation by function: | | |
|---|---|---|---|
| | **Exponential 2 terms** | **Exponential 1 term** | **Polynomial the grade 3** |
| SSE | 8063 | 5.212e+004 | 5074 |
| R-square | 0.9984 | 0.9899 | 0.999 |
| Adjusted R-square | 0.9973 | 0.9882 | 0.9983 |
| RMSE | 44.9 | 93.21 | 35.62 |

*B. Inverse Characteristic*

To determine the inverse characteristic considered working range of the sensor as a meeting of intervals [0.....2500] mV. It has been switched back to the working environment Matlab/Cftool.

Characteristic approximation result is shown in figure 7. Sensory function describing the characteristic element is expressed:

$$x = 1589 \cdot e^{-0.001786 \cdot U} + 567 \cdot e^{-0.0004792 \cdot U} \; [mm] \quad (3)$$

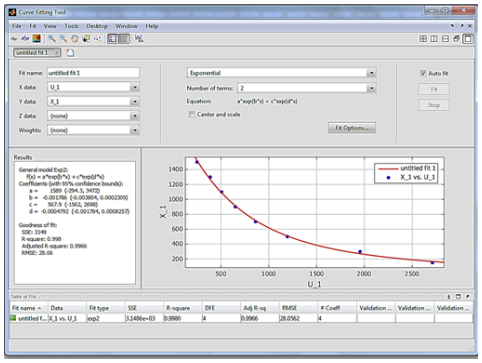

**Fig. 7 Approximation characteristic x = x(U)**

International Journal of Emerging Technology and Advanced Engineering
Website: www.ijetae.com (ISSN 2250-2459, ISO 9001:2008 Certified Journal, Volume 5, Issue 1, January 2015)

Table 4 presents the comparison of statistical indicators to approximate refereritoare previous feature. It is noted that the polynomial approximation is superior statistical indices exponential approximation.

**Table 4,**
**Approximation of the characteristic**

| | Approximation by function: | | |
|---|---|---|---|
| | **Exponential 2 terms** | **Exponential 1 term** | **Polynomial the grade 3** |
| SSE | 3149 | 1.543e+004 | 1204 |
| R-square | 0.998 | 0.9904 | 0.9993 |
| Adjusted R-square | 0.9966 | 0.9888 | 0.9987 |
| RMSE | 28.06 | 50.71 | 17.35 |

## III. Location An Obstacle And Experimental Stand

Next stage experimental analysis followed two operational objectives:

- The possibility of determining the existence of an obstacle based on information from sensors IR;
- The possibility to position / orientation of the obstacle with respect to an axis generally attached sensory system used.

The sensory system is built around SHARP GP2Y0A02YK0F sensors for which high functional feature.

Structural diagram of the experimental program carried out is shown in Figure 8.

The three elements are arranged in a linear sense.

In figure 9 is shown a detail of the stand made and in figure 10 is a schematic diagram of power supply elements and processing sensory information, where C1 = C2 = C3 = 1000µF, C4 = 660µF.

We have introduced these capacitors to eliminate voltage variation according to the documentation sensor [19].

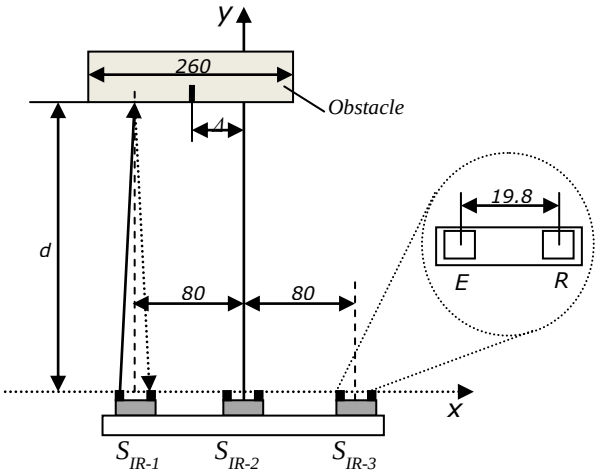


a)

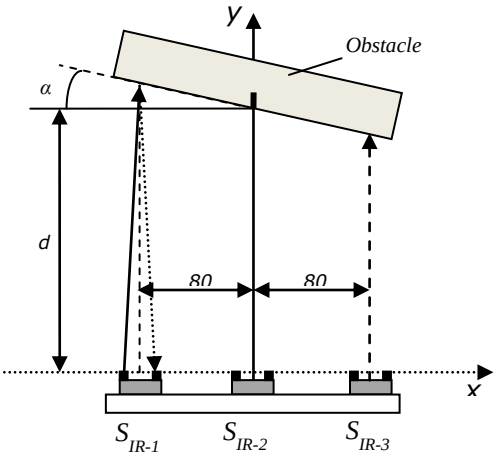


b)

**Fig. 8(a,b), Structural diagram of the experimental program stand**

International Journal of Emerging Technology and Advanced Engineering
Website: www.ijetae.com (ISSN 2250-2459, ISO 9001:2008 Certified Journal, Volume 5, Issue 1, January 2015)

During the experiments considered inverse characteristic equation IR sensor described by the expression:

$$d_x = -116 \cdot U^3 + 371.2 \cdot U^2 - 512.4 \cdot U + 569.1\, mm \quad (4)$$

Where U[mV] sensory element is an analog signal, and the characteristic equation in the form:

$$d_x = 1505 \cdot e^{-0.001836 \cdot U} + 625.4 \cdot e^{-0.000545} \; mm \quad (5)$$

Where U[mV] is the analog signal of the sensing element.

We watched comparing the obtained equations.

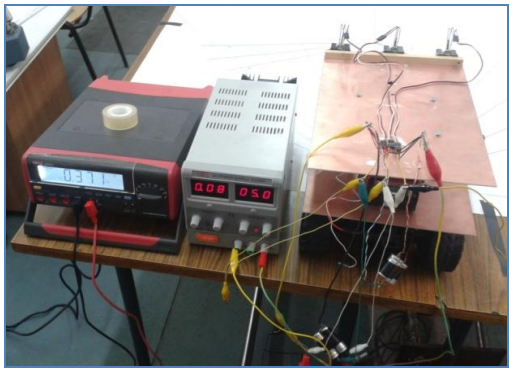

**Fig. 9, Details of exhibition stand**

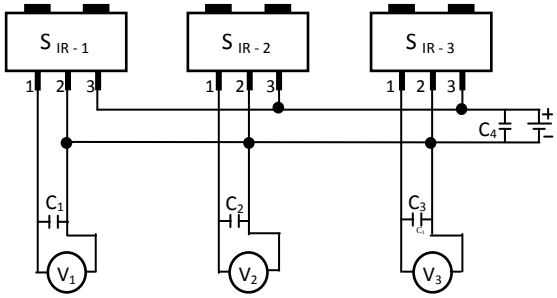


**Fig. 10, Wiring diagram of the experimental setup**

*A. Location of an Obstacle in the Working Scene*

Set of measurements was performed on a rectangular obstacle positioned at distances of 500 mm, 1000 mm and 1500 mm to the plane of the sensor elements. In Table 5 the values of information processed for 2 sensors (S IR-1, S IR-3), where μ is the average voltage measured at the sensor output and σ is the density of probability.

**Table 5,**
**Processed values**

| | S IR-1 | | S IR-3 | |
|---|---|---|---|---|
| Distance [mm] | $\mu_1$ [mV] | $\sigma_1$ | $\mu_3$ [mV] | $\sigma_3$ |
| 500 | 1198 | 2.28 | 1185.8 | 1.923 |
| 1000 | 577.4 | 1.673 | 588.8 | 1.483 |

Based on these values is presented in figure 11 versus the density of probability associated experiments conducted.

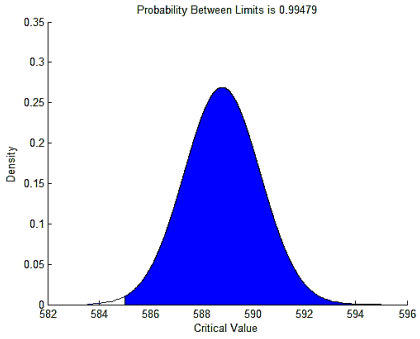


**a)**

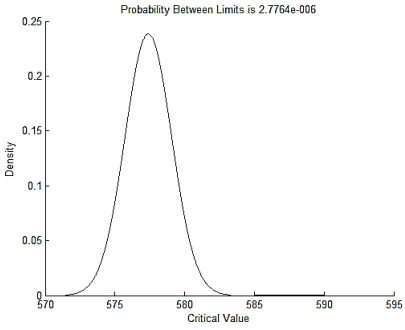


**b)**

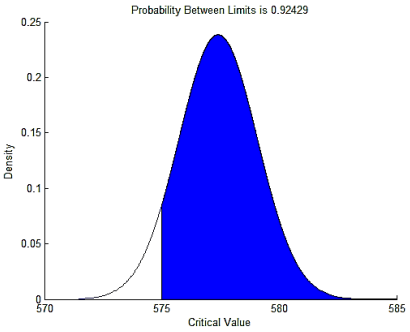


**c)**

International Journal of Emerging Technology and Advanced Engineering
Website: www.ijetae.com (ISSN 2250-2459, ISO 9001:2008 Certified Journal, Volume 5, Issue 1, January 2015)

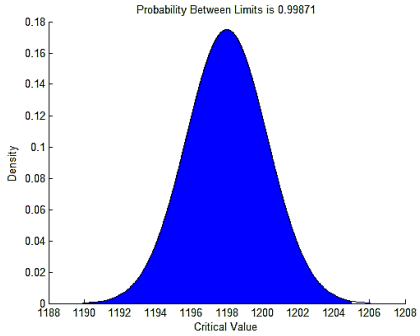


**d)**

**Fig. 11(a,b,c,d), The density of probability**

*B. Calculation Parameters of an Obstacle Location*

The next set of tests was to determine the location of the obstacle parameters in scene analyzed.

We present the case of tests carried out centrally rectangular obstacle to the distance axis system $Y_0$ = 1000 mm and rotated through an angle α = 30⁰ in clockwise rotation were determined distances measured by the three sensors (Table 6).

**Table 6**
**Distance measured by three sensors**

| $d_x - S_{IR-1}$ [mm] | $d_x - S_{IR-2}$ [mm] | $d_x - S_{IR-3}$ [mm] |
|---|---|---|
| 1133.944 | 1063.436 | 968.9623 |

The equation of the straight line that approximates the position of an obstacle in plan (Figure 12) is described by the equation:

$$Y = -1.031 \cdot x + 1055 \quad (6)$$

The true coefficients were calculated in terms of a confidence coefficient 95 %, Table 7.

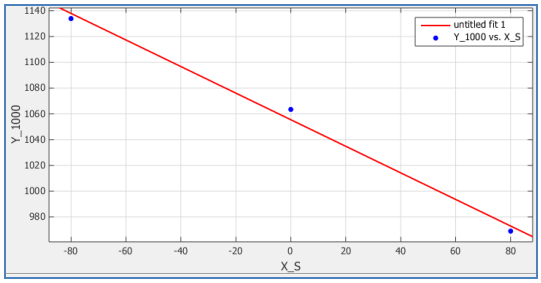


**Fig. 12, Approximation equation was situated obstacle**

**Table 7**
**Value of regression coefficient**

| | |
|---|---|
| SSE | 95.73 |
| R_square | 0.993 |
| Adjusted R-square | 0.986 |
| RMSE | 9.784 |

It is found that the positioning error of the obstacle is:

$$\varepsilon_{OY} = \frac{1000 - 1055}{1000} = \frac{-55}{1000} = -0.055 \quad (7)$$

and orientation error:

$$\varepsilon_{OY} = \frac{30^0 - 46.8266^0}{30^0} = \frac{-16.8266^0}{30^0} = -0.52992 \quad (8)$$

For a rectangular obstacle positioned centrally with respect to the system axis at a distance of $Y_0$ = 1000 mm and rotated at an angle α= $30^0$ in the opposite direction of the clockwise were determined distances measured by the three sensors (Table 8, Table 9).

Equation that approximates a straight position of the obstacle plan (Figure 13 (a)) is described by the equation:

$$Y = -0.3303 \cdot x + 962.6 \quad (9)$$

**Table 8,**
**Distance measured by three sensors**

| $d_x - S_{IR-1}$ [mm] | $d_x - S_{IR-2}$ [mm] | $d_x - S_{IR-3}$ [mm] |
|---|---|---|
| 926.3707 | 982.2246 | 979.3481 |

**Table 9,**
**Value of regression coefficient**

| | |
|---|---|
| SSE | 577.1 |
| R_square | 0.7076 |
| Adjusted R-square | 0.4151 |
| RMSE | 24.03 |

Compared to the straight line equations are presented for the same position of the obstacle in the mirror orientations, figure 13.

International Journal of Emerging Technology and Advanced Engineering
Website: www.ijetae.com (ISSN 2250-2459, ISO 9001:2008 Certified Journal, Volume 5, Issue 1, January 2015)

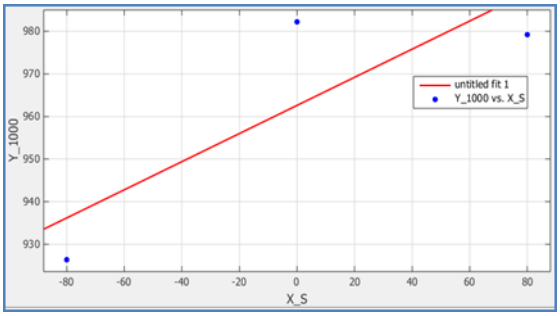


**a)**

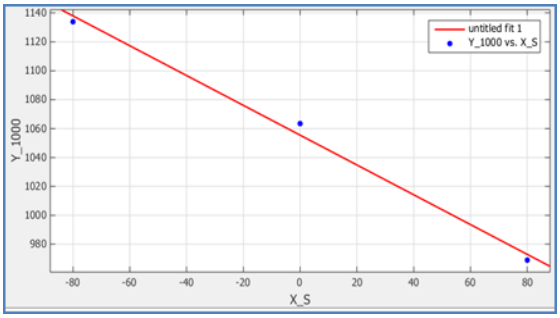


**b)**

**Fig. 13 (a,b), Approximation equation was situated obstacle**

The true coefficients were calculated in terms of a confidence coefficient of 95%. It is noted that the obstacle is the position error:

$$\varepsilon_{OY} = \frac{1000 - 962.6}{1000} = \frac{37.4}{1000} = 0.0374 \qquad (10)$$

and orientation error:

$$\varepsilon_{OY} = \frac{30^0 - 18.28766^0}{30^0} = \frac{11.71234^0}{30^0} = 0.39 \qquad (11)$$

## IV. Conclusions

Experiments allowed enunciation following conclusions:

- The location of an obstacle with an IR sensor is dependent on the surface condition parameters barriers and reflective.
- Direct feature sensory element is similar to the IR sensor documentation [19], [8].
- Sharp sensing element GP2Y0A21YK working parameters used in the [0…1200 mm].
- Statistical analysis and determination of the probability density allows subsequent analysis stage work.
- The direct and inverse characteristic we examined the use of two areas defined in relation to the maximum output range.
- Sensory input feature is non-linear, with a maximum output signal at a distance d0 between obstacle and sensor.

*Acknowledgments*

This paper is supported by the Sectorial Operational Programme Human Resources Development (SOP HRD), ID134378 financed from the European Social Fund and by the Romanian Government.

## REFERENCES

[1] M. Mohammad, "Posssibilistic Sonar Modeling and Localization for Mobile Robot", Ph.D. thesis, Concordia University Montreal, Quebec, August 1997.

[2] C. Cocaud and A. Jnifene, "Environment mapping using probabilistic quadtree for guidance and control of autonomous mobile robots", Dep. Of Mech. Eng., Kingston, Canada, 05547019.pdf.

[3] L. Limei and colab., "A map building method based on uncertain information of sonar sensor", The 9th International Conference for Young Computer Scientists, p.1738 – 1742, 2008.

[4] A. Mondoc, "Theoretical and Experimental Analysis of the Random Aspects in the Work Scene of a Mobile Robot", Ph.D. thesis, Politehnica University of Timisoara, 2014.

[5] J. Dixon and O. Henlich, "Mobile Robot Navigation", Imperial College, 10 June 1997.

[6] J. Borenstein and L. Feng, "Measurement and correction of systematic odometry errors in mobile robots", IEEE Transactions on Robotics and Automation 12, 1996.

[7] M. Han, and S. Rhee, "Navigation control for a mobile robot", Journal of Robotics Systems 11(3), 169–179, 1994.

[8] V. Krys, T. Kot, J. Bajak and V. Mostyn, "Testing and calibration of IR proximity sensors", Acta Mechanica Slovaca, 3/2008.

[9] H. R. Everett, "Sensors for Mobile Robots: Theory and Application", A K Peters, Ltd., Wellesley, MA, ISBN 1-56881-048-2, 1995.

[10] A. Sabatini, V. Genovese, E. Guglielmelli, A. Mantuano, G. Ratti, and P. Dario, "A low-cost, composite sensor array combining ultrasonic and infrared proximity sensors", International Conference on Intelligent Robots and Systems, Pittsburgh, Pennsylvania, 3:120-126, August 5-9 1995.

[11] V. Colla, A.M. Sabatini, "A composite proximity sensor for target location and color estimation", in: Proceedings of the IMEKO Sixth International Symposium on Measurement and Control in Robotics, Brussels, pp. 134–139, 1996.

[12] P.M. Vaz, R. Ferreira, V. Grossmann, M.I. Ribeiro, "Docking of a mobile platform based on infrared sensors", in: Procee677 dings of the 1997 IEEE International Symposium on Industrial Electronics, Vol. 2, Guimaraes, Portugal, pp. 735–740, July 1997.

[13] L. Korba, S. Elgazzar, T. Welch, "Active infrared sensors for mobile robots", IEEE-Transactions on Instrumentation and Measurement 2 (43) 283–287, 1994.

[14] G. Benet, F. Blanes, J.E. Simo, P. Perez, "Using infrared sensors for distance measurement in mobile robots", Journal of Robotics and Autonomous Systems, vol. 10, pp. 255-266, 2002.

[15] T. Mohammad, "Using Ultrasonic and Infrared Sensors for Distance Measurement", World Academy of Science, Engineering and Technology Vol:3 2009-03-26.

[16] P.M. Novotny, N.J. Ferrier, "Using infrared sensors and the Phong illumination model to measure distances", in: Proceedings of the International Conference on Robotics and Automation, Vol. 2, Detroit, MI, USA, pp. 1644–1649, April 1999.

[17] http://www.sierra.ro/Senzor-analog-de-distanta-10---80-cm-(SHARP)-p5320p.html.

[18] F. Gorunescu and M. Gorunescu, "Exploratory analysis and processing simulations in Mathlab" "Blue Publishing, Cluj-Napoca, 2013.

[19] http://www.sharpsma.com/webfm_send/1487